

Supporting information

Multicomponent solid forms of antibiotic Cephalexin towards improved chemical stability

T. K. S. Fayaz,^a Vasanthi Palanisamy,^a Palash Sanphui,^{*a} Vladimir Chernyshev^{*b,c}

^aDepartment of Chemistry, Faculty of Engineering and Technology, SRM Institute of Science and Technology, Chennai, Tamil Nadu 603203, India. E-mail: palashi@srmist.edu.in

^bDepartment of Chemistry, M. V. Lomonosov Moscow State University, 1-3 Leninskie Gory, Moscow 119991, Russian Federation. E-mail: vladimir@struct.chem.msu.ru

^cA. N. Frumkin Institute of Physical Chemistry and Electrochemistry RAS, 31 Leninsky Prospect, Moscow 119071, Russian Federation

Table of contents

1. Table S1. Hydrogen bond geometry.....
2. Fig. S1. PXRD comparison of CPX hydrate with its calculated XRD patterns.....
3. Fig. S2. The Rietveld plot of CPX–SER cocrystals.....
4. Fig. S3. Hydrogen bonding in CPX hydrate.....
5. Fig. S4. Molecular packing of CPX–SER cocrystal.....
6. Fig. S5. Overlay of PXRD of CPX–DHB salt hydrate with its calculated X-ray patterns
7. Fig. S6. PXRD comparison of CPX multicomponent solids under humidity conditions.....
8. Fig. S7. HPLC chromatogram comparison of CPX hydrate with standard CPX sample.....
9. Fig. S8. HPLC chromatograms CPX and CPX binary solids following acid hydrolysis.....

Table S1. Hydrogen bond geometry ($\text{\AA}/^\circ$)

CPX binary solids	D-H \cdots A	D-H/ \AA	H \cdots A/ \AA	D \cdots A/ \AA	D-H \cdots A/°	Symmetry code
CPX-SER	N2-H2 \cdots O4	0.86	2.24	2.9792(4)	144	x,y,-1+z
	N3-H3A \cdots O1	0.89	1.73	2.5844(4)	159	1/2+x,1/2-y,-z
	N3-H3B \cdots O5	0.89	2.08	2.8598(4)	145	1-x,1/2+y,3/2-z
	N3-H3C \cdots O5	0.89	2.02	2.6942(4)	132	1-x,1/2+y,1/2-z
	N4-H4A \cdots O6	0.89	1.92	2.6659(4)	141	1/2-x,-y,-1/2+z
	N4-H4B \cdots O2	0.89	2.14	2.9803(4)	158	-
	N4-H4C \cdots O2	0.89	2.03	2.8657(4)	156	x,y,1+z
	O7-H7 \cdots O3	0.82	2.31	2.9770(4)	140	x,y,1+z
	C1-H1 \cdots O3	0.98	2.49	3.1797(5)	128	x,y,1+z
	C5-H5 \cdots O3	0.98	2.54	3.2274(5)	127	x,y,1+z
	C10-H10 \cdots O4	0.98	2.25	3.1225(5)	148	x,y,1+z
	C16-H16 \cdots O5	0.93	2.16	3.0851(4)	174	1-x,1/2+y,3/2-z
	C18-H18 \cdots O6	0.98	1.86	2.8106(4)	163	x,y,-1+z
CPX-DHB . H ₂ O	O2-H2 \cdots O5	0.89	1.70	2.5699(1)	167	2-x,-1/2+y,1-z
	N2-H2A \cdots O9	0.83	2.32	3.1048(2)	156	1+x,y,z
	N3-H3A \cdots O2	0.89	2.30	3.0520(2)	143	-1+x,y,z
	N3-H3B \cdots O7	0.95	1.74	2.6720(1)	167	-
	N3-H3C \cdots O5	0.89	2.55	3.1982(2)	130	-
	N3-H3C \cdots O1	0.89	1.97	2.7153(1)	141	2-x,1/2+y,1-z
	O5-H5A \cdots O3	0.81	2.14	2.8914(2)	155	-1+x,y,z
	O5-H5B \cdots O6	0.93	1.77	2.6591(1)	159	-
	C1-H1 \cdots O9	0.98	2.36	3.2431(2)	149	1+x,-1+y,z
	C10-H10 \cdots O1	0.98	2.60	3.0112(2)	105	2-x,1/2+y,1-z

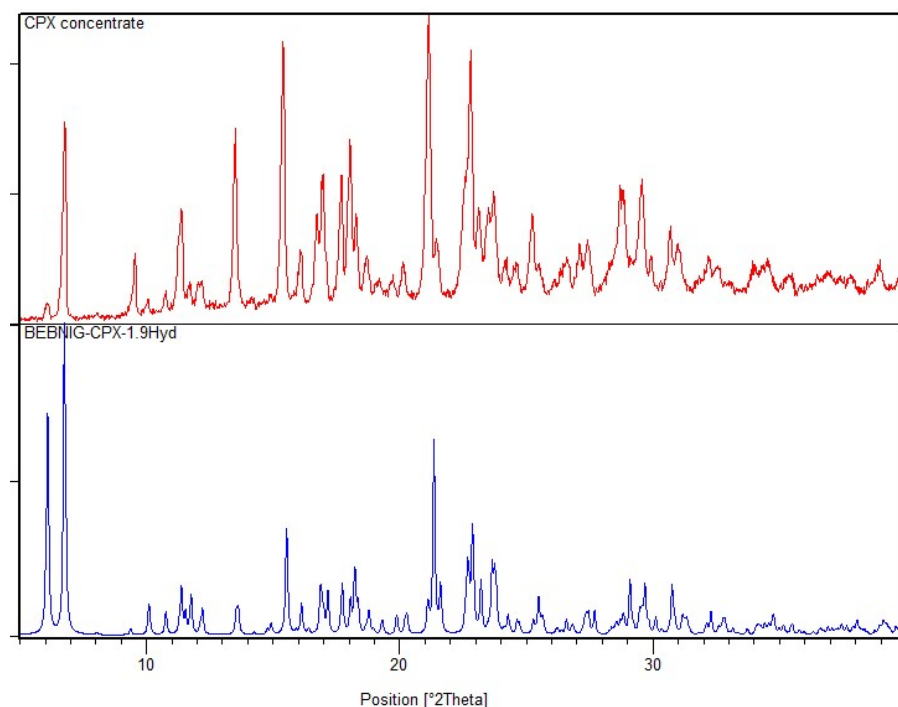


Fig. S1. PXRD comparison of CPX (extracted from commercialized tablets) with the calculated XRD pattern of CPX-1.9 hydrate from its crystal structure (CCDC refcode: BEBNIG). Peak to peak match confirms its bulk phase purity.

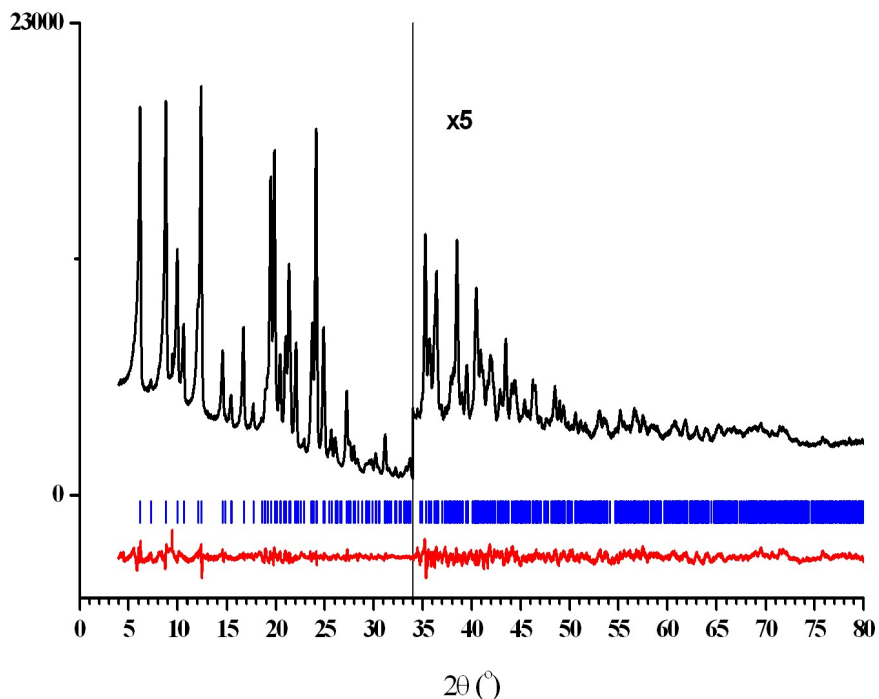


Fig. S2. The Rietveld plot after the final bond-restrained refinement for CPX–SER, showing the experimental and difference diffraction profiles as black (top) and red (bottom) curves, respectively. The vertical blue bars correspond to the calculated positions of the Bragg peaks.

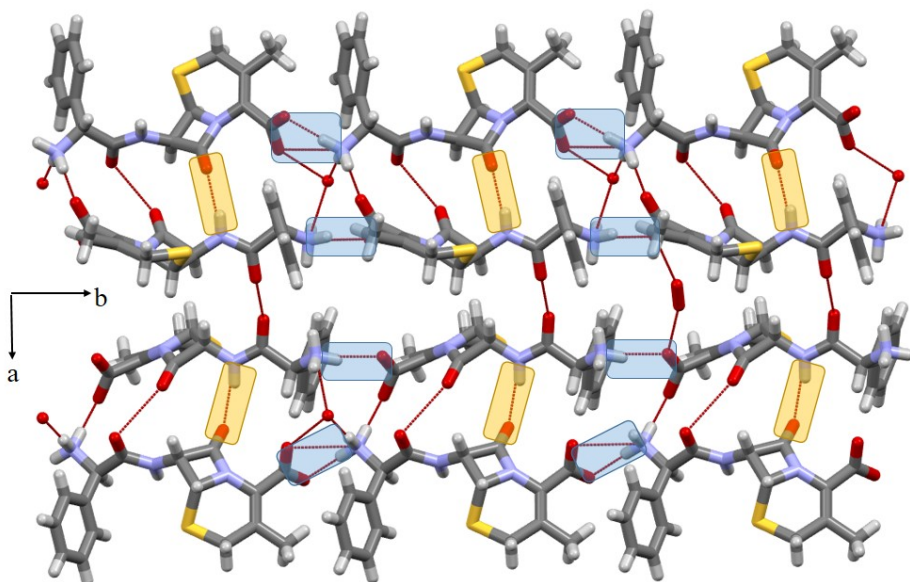


Fig. S3. CPX molecules form $\text{N}^+–\text{H}···\text{O}^-$ hydrogen bonded 1D chain between carboxylate and ammonium ions along the b axis, whereas $\text{N}–\text{H}···\text{O}$ hydrogen bond (amide NH/ and lactam CO) and $\text{O}···\text{O}$ short contacts along the a axis resulted 2D sheet structure in CPX hydrate.

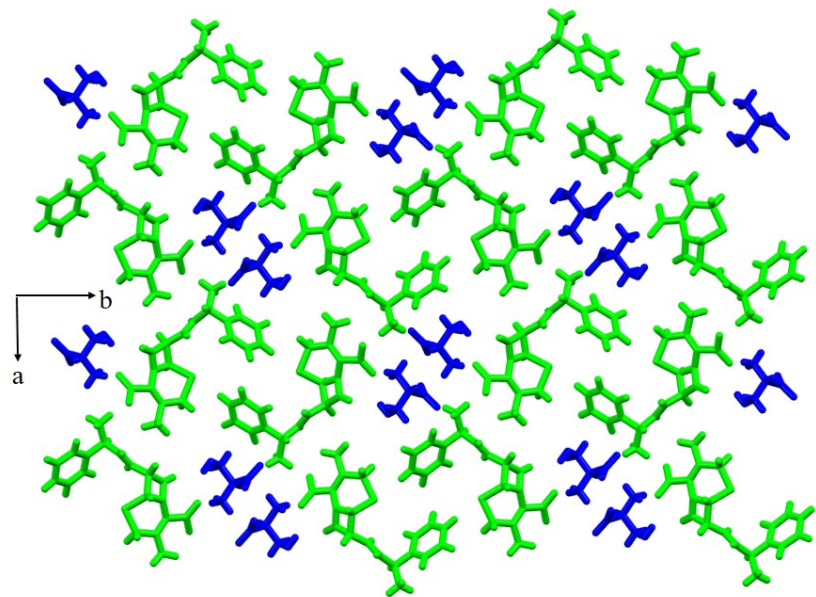
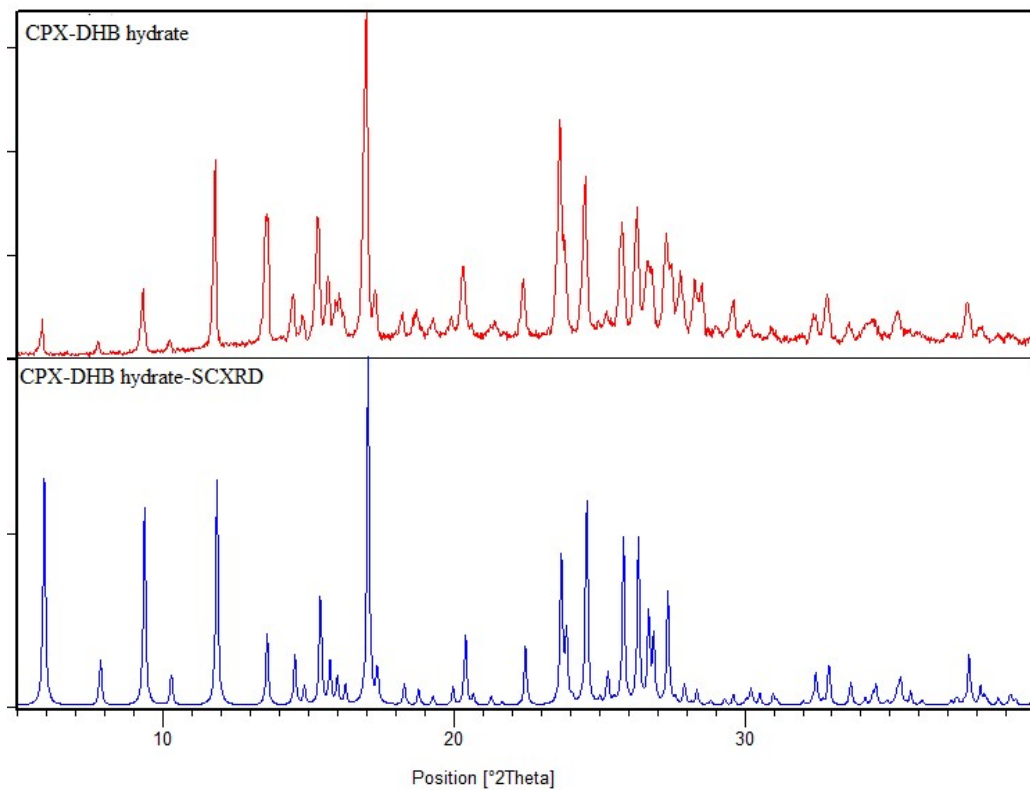
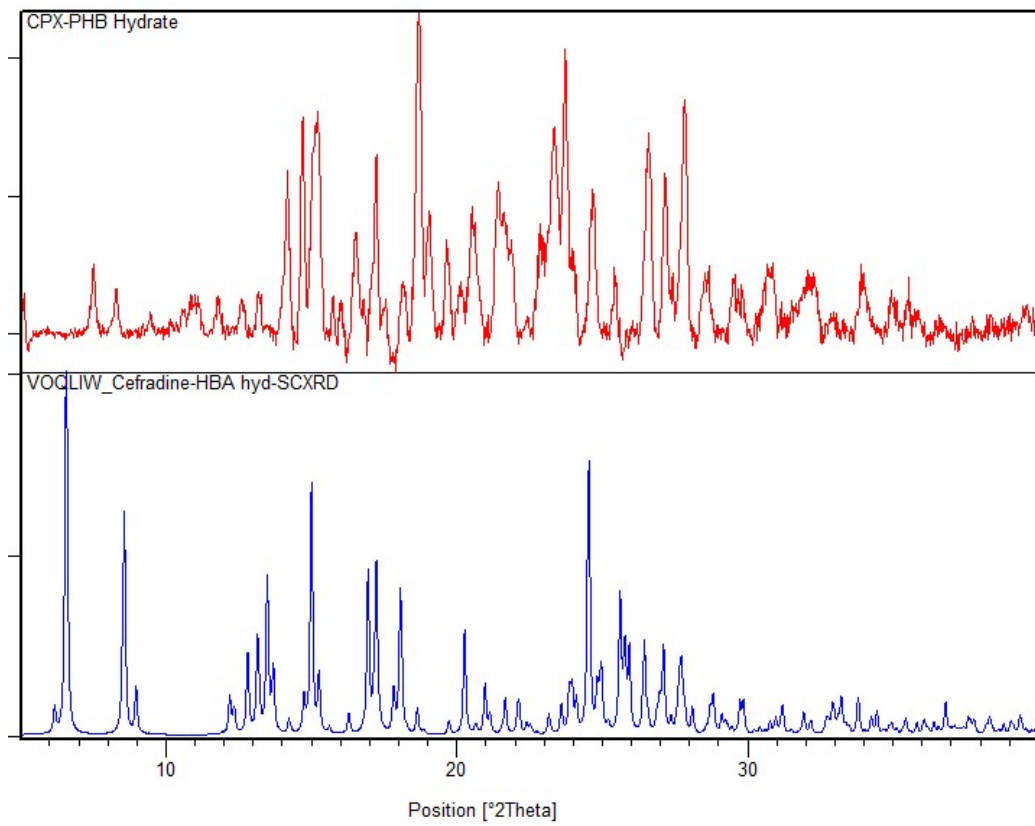


Fig. S4. Molecular packing of CPX–SER cocrystal viewed down the c axis represent host (CPX, green trace)-guest (SER, blue trace) assembly.

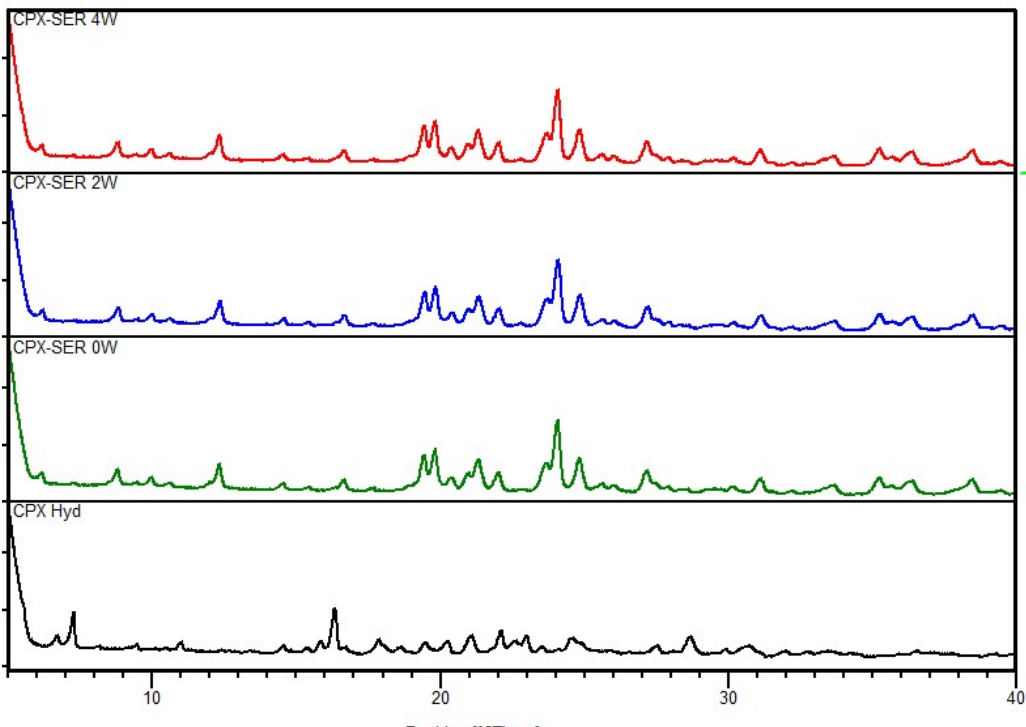
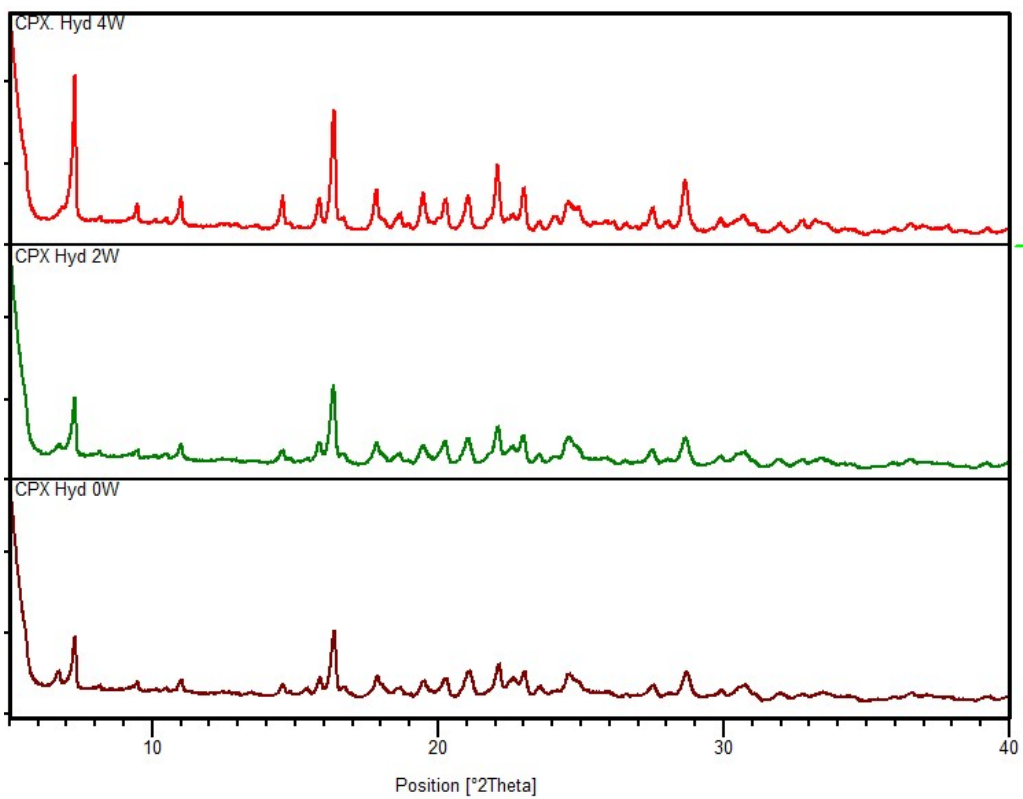


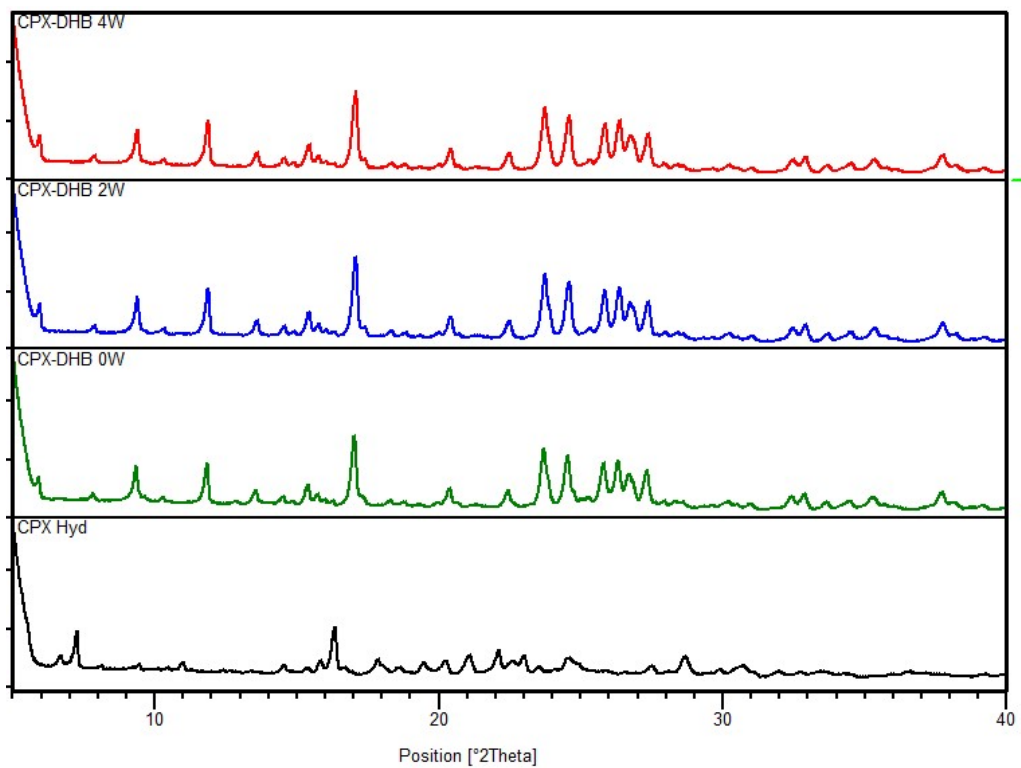
(a)



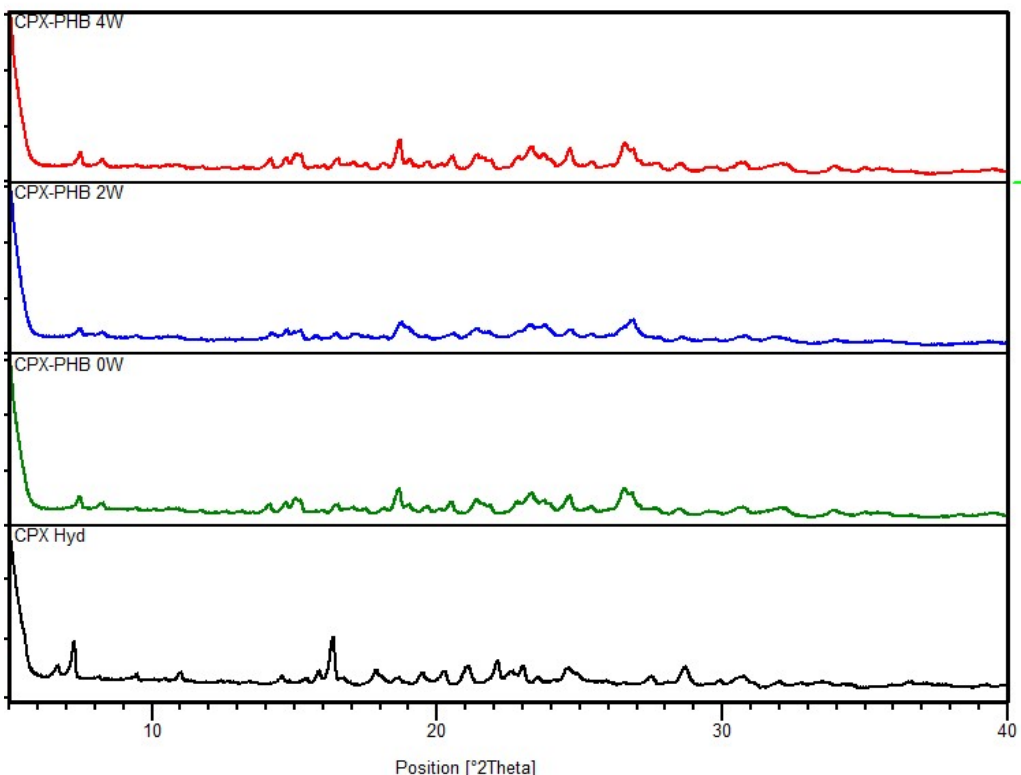
(b)

Fig. S5. a) Overlay of PXRD (red trace) of CPX–DHB salt hydrate with its calculated X-ray patterns (blue trace) from crystal structure confirms the bulk phase purity. b) Overlay of PXRD pattern of CPX–PHB hydrate with the simulated XRD pattern of VOQLIW indicated partial match that suggested possibility of multiple phases may be present in the sample.





(c)



(d)

Fig. S6. PXRD comparison of a) CPX Hyd, b) CPX–SER, c) CPX–DHB, and d) CPX–PHB upto 4 weeks in 35 ± 5 °C and $75\pm 5\%$ relative humidity that confirmed the physical stability of all the multicomponent solids as CPX hydrate.

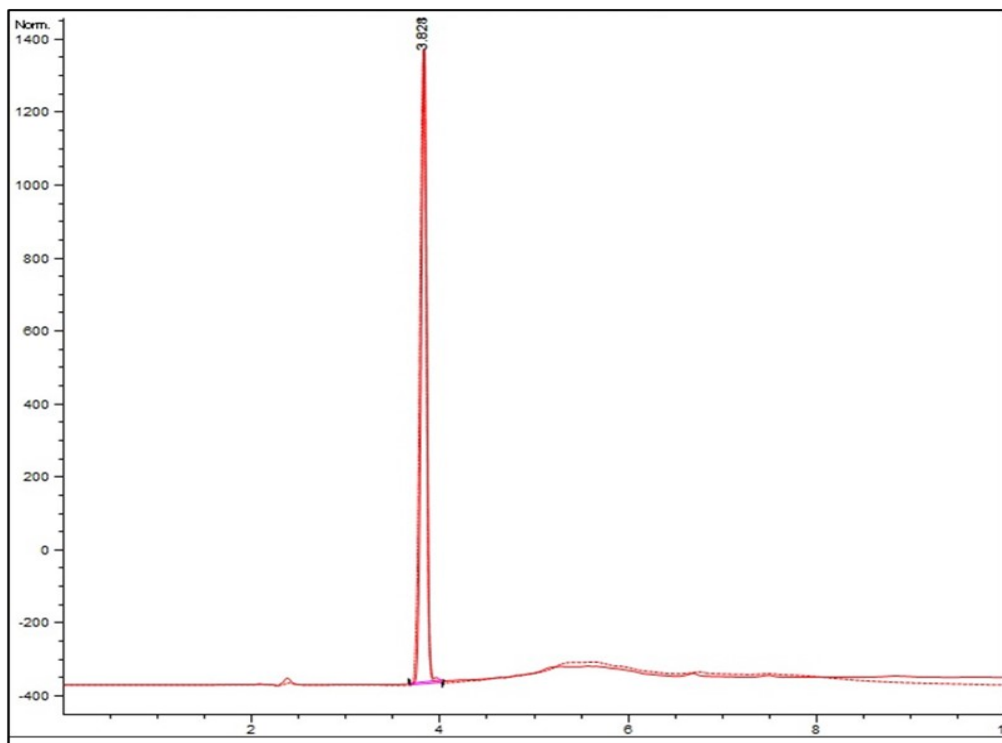
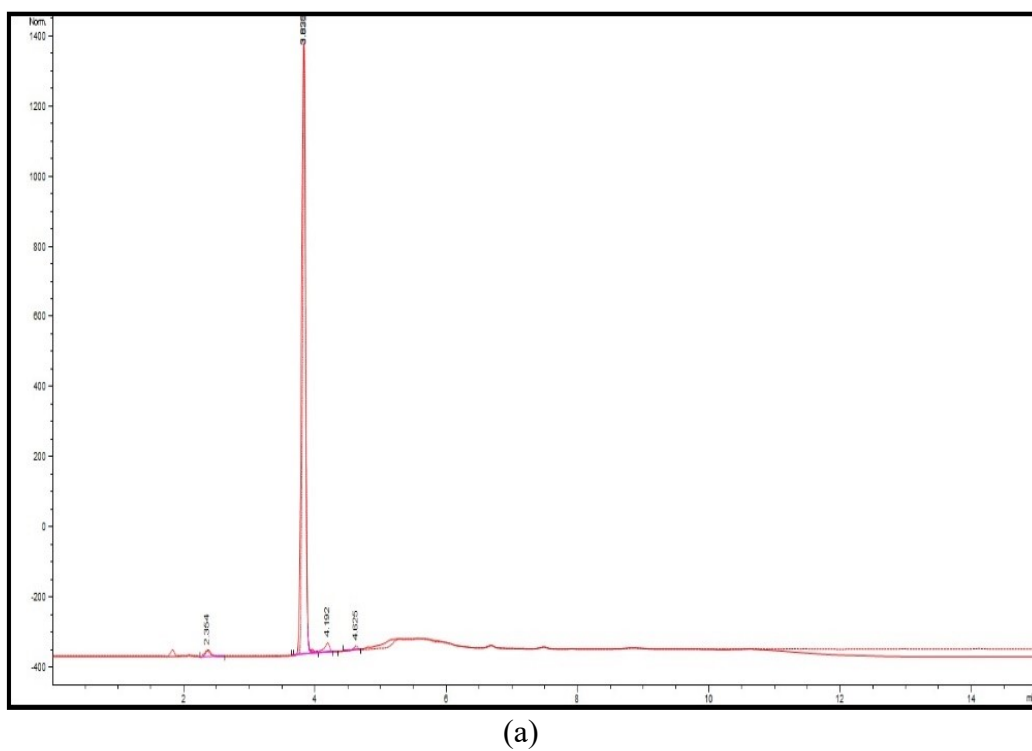
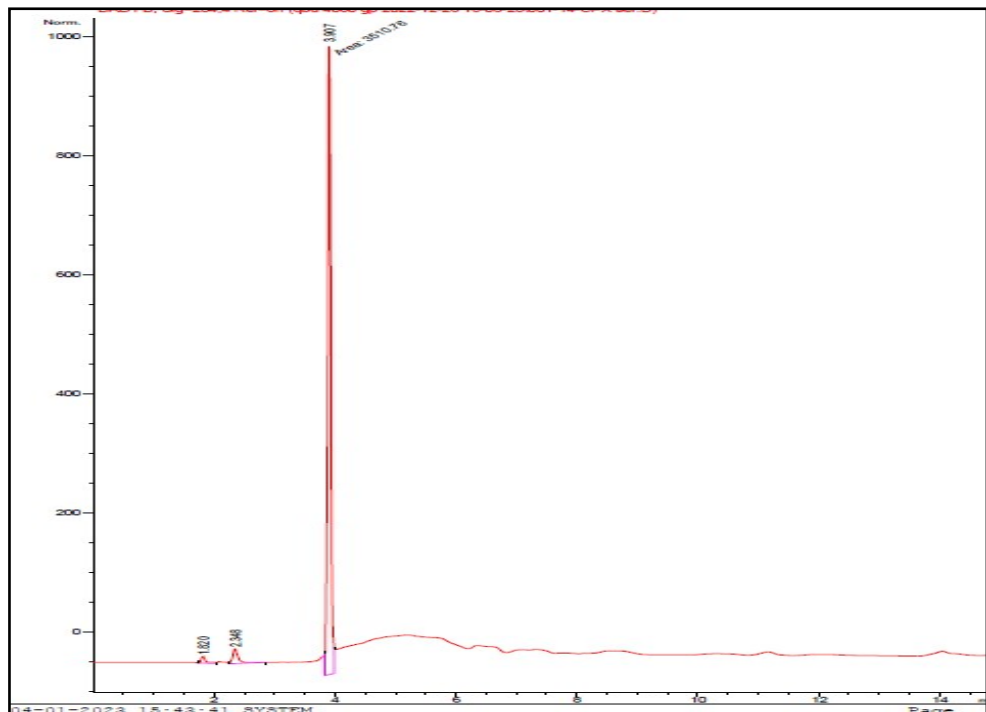
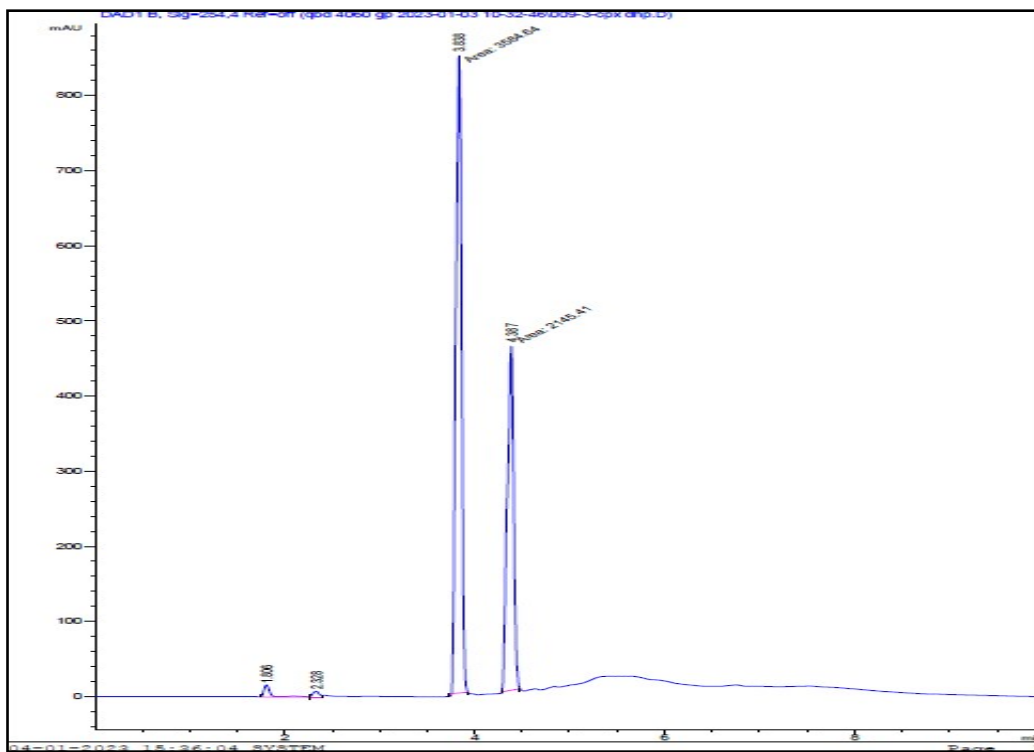


Fig. S7. HPLC overlay of CPX standard and CPX Sample used for cocrystallization





(b)



(c)

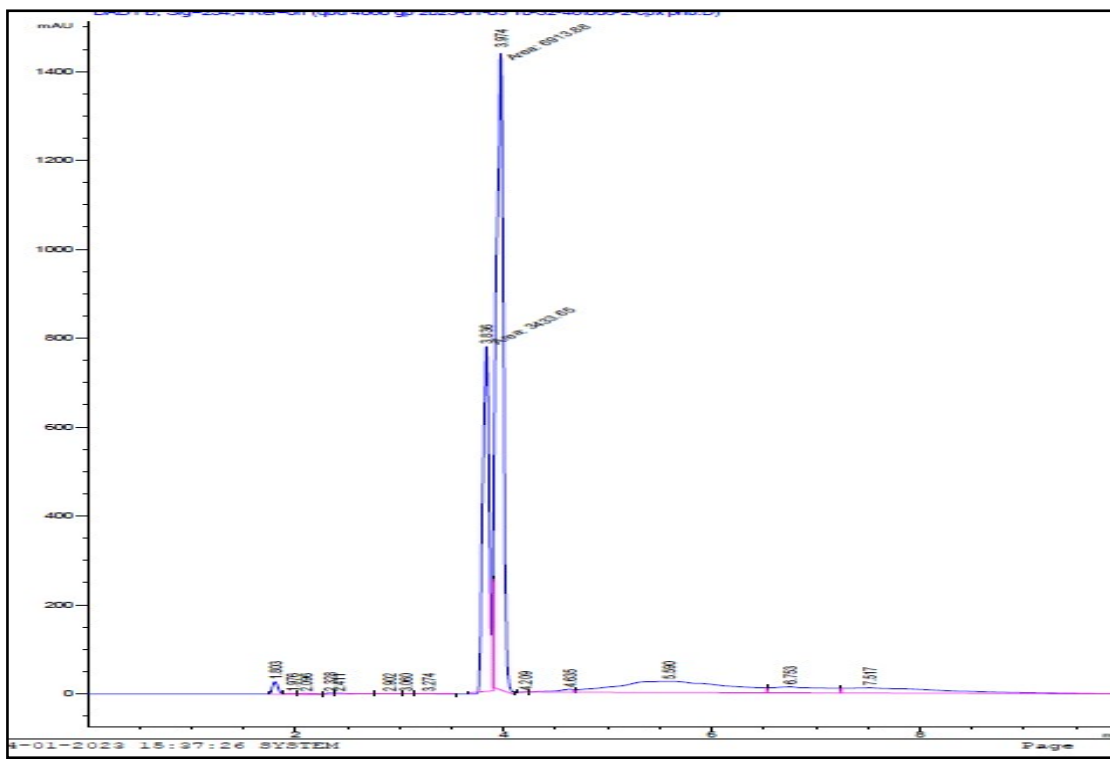


Fig. S8. HPLC chromatogram of a) CPX, b) CPX-SER, c) CPX-DHB and d) CPX-HBA following acid hydrolysis.